

Microscopic Simulation of Reaction-Diffusion
Processes and Applications to Population Biology
and Product Marketing

Eldad Bettelheim and Benny Lehmann

October 1998

1 Introduction

Reaction-diffusion processes are the subject of much research [7] [2] [25] [15] [9] [23], a reaction-diffusion process occurs as reactants in a solution diffuse in the liquid and react amongst themselves. A common approach to reaction-diffusion processes is to consider the density fields of the different reactants participating in the reactions. This approach stands in contrast to the more naive approach of tracking the locations of the different reactants, or computing the wave functions of the different reactants. Whatever approach is taken the interest in a reaction-diffusion system is usually in its spatio-temporal evolution. The density field approach is especially adept for this purpose, since the actual location of specific reactants is, usually of no interest. In the density fields approach the spatio-temporal evolution is modeled through partial differential equations (PDE's).

Another approach to reaction-diffusion processes that we have suggested is the microscopic approach. In this approach we consider the number of reactants at discrete lattice points, where the lattice models space. The main difference from the density field approach is that rather than using continuous densities in a continuous space as in the density field approach, we use discrete densities in discrete space.

The microscopic simulation approach is closer to the real simulated system when there are only trace densities of the different reactants. This is because it is in this situation that the discrete nature of the reactants comes into play. Consequently the PDE approach describes the system with less accuracy than when there are many reactants.

Reaction-Diffusion processes are not restricted to describing chemical systems. Indeed reaction-diffusion processes have even been used extensively in population biology [21]. We have also used a reaction-diffusion model in a marketing context. We have seen that discretization was crucial in the behavior of the modeled market. Thus showing that microscopic simulation could be of use to researchers who need to model real-life systems.

2 The Density Field Approach

2.1 Analytical approach

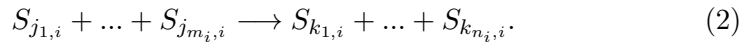
In this section we shall describe the density field approach [21]. As mentioned in the introduction, The density field approach considers the evolution of the the density fields of the reactants participating in the reaction-diffusion system. Say that reactants numbered 1 to n are participating in

the reactions (possibly as reactants or as products). Then we could label the density fields by $\rho_i(\vec{x}, t)$. The density is defined as:

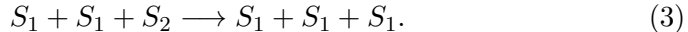
$$\rho_i(\vec{x}, t) = \frac{1}{n_0} \lim_{V(A) \rightarrow 0} \frac{N(i, A, \vec{x}, t)}{V(A)} \quad (1)$$

A is a box, $N(i, A, \vec{x}, t)$ is the number of molecules of type i that are in the box A located about \vec{x} . $V(A)$ is the volume of box A. And n_0 is a constant that serves the same purpose as Avogadro's constant. It should be noted that, if a smooth density function is wanted, the limit should not be taken to zero literally, but rather should be taken down to a scale much larger than one that shows the discretization of the reactants, and much smaller than the scale of the macroscopic spatial patterns.

Let us assume l possible reactions, where reaction i is of the form:



Where S_r denotes the r^{th} reactant. As an example of such a reaction let us look at:



this reaction is of the form (2). An interpretation of this reaction is that two reactants of species 1 can cause a reactant of species 2 to turn into a reactant of species 1. Let us consider a system which has two chemicals, which we shall denote, as usual, by S_1 and S_2 . These chemicals can diffuse with diffusion coefficients of D_1 and D_2 respectively. These chemicals can also react according to the reaction scheme (3).

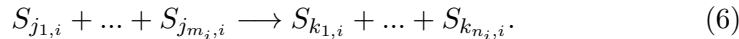
The time evolution of the fields, $\rho_1(\vec{x}, t)$ and $\rho_2(\vec{x}, t)$, is given by:

$$\frac{\partial \rho_1}{\partial t} = D_1 \nabla^2 \rho_1 + k \cdot \rho_1^2 \rho_2 \quad (4)$$

$$\frac{\partial \rho_2}{\partial t} = D_2 \nabla^2 \rho_2 - k \cdot \rho_1^2 \rho_2 \quad (5)$$

Equation 4 has two terms on the right hand side (RHS), let us turn our attention first to the second term. The term contains the expression $\rho_1^2 \rho_2$. This is proportional to the probability that two reactants of species 1 and one reactant of species 2 meet in a small region in space (the volume of that region is a given). The coefficient k is the probability that, once the reactants met in the small region in space, they will react with one another. The Diffusion term is the familiar term, which originates from the "random walk" of the reactants.

In general, when we have l reactions, each of the form (2),



If we denote by $\mathbf{N}_{p,r}$ the number of reactants of species \mathbf{r} created or annihilated by reaction \mathbf{p} then we have the following rate equations:

$$\frac{\partial \rho_r}{\partial t} = \sum_{p=1}^l k_p N_{p,r} \prod_{s=1}^{s=m_p} \rho_{j_{s,p}} + D_r \nabla^2 \rho_r \quad (7)$$

2.2 Simulation by finite difference

The former section introduced the formalism of the density field approach which is essentially analytic, but there is no data structure on a computer that can hold an arbitrary continuous field. So space is discretized in the computer simulation. The other problem which arises is the need to integrate the differential equations over time. This is done again by discretization but the solution now is to discretize time. The most naive way to integrate using the differential equation is by Euler integration. This method's main drawback is the computation time that it requires to get accurate results. But fundamentally it is no different than other more sophisticated methods such as the runga-cutta method. We shall outline this finite difference approach using Euler integration below.

In the finite difference approach using Euler integration one replaces the fields $\rho_r(\vec{x}, t)$ with $\vec{x} \in R^d$ and $t \in R$ by $\rho_r^*(\vec{x}, t)$ where $\vec{x} \in \omega^d$ $t \in \omega$ (ω being the natural numbers). Let us suppose that the following equations hold for the fields ρ_r :

$$\frac{\partial \rho_r}{\partial t} = f(\rho_1, \dots, \rho_n) + D \nabla^2 \rho_r, \quad (8)$$

In order to make this transition from ρ to ρ^* , space is conceptually divided to a discrete d-dimensional lattice of spacing Δx and time is divided to a discrete 1-dimensional lattice (actually a series) of spacing Δt . Now the aim is to make the following equality be a good approximation:

$$\rho_r^*((n_1, n_2, \dots, n_d), m) \approx \rho_r(\Delta x \cdot (n_1, n_2, \dots, n_d), m \cdot \Delta t) \quad (9)$$

The way to make this approximation good is to let Δx and Δt be small and to let ρ^* follow the dynamics:

$$\begin{aligned} \rho_r^*(\vec{x}, t + 1) - \rho_r^*(\vec{x}, t) &= \Delta t \cdot f(\rho_1^*, \dots, \rho_n^*) + \frac{D_r \Delta t}{\Delta x^2} \\ &(\rho_r^*(\vec{x} + (1, 0, \dots, 0), t) + \rho_r^*(\vec{x} + (-1, 0, \dots, 0), t) + \end{aligned}$$

$$\begin{aligned} & \rho_r^*(\vec{x} + (0, 1, \dots, 0), t) + \rho_r^*(\vec{x} + (0, -1, \dots, 0), t) + \dots \\ & \rho_r^*(\vec{x} + (0, 0, \dots, 1), t) + \rho_r^*(\vec{x} + (0, 0, \dots, -1), t) - 2d\rho_r^*(\vec{x}, t) \end{aligned} \quad (10)$$

The first term on the right hand side of the equation is the first order approximation of the difference between $\rho_r(\vec{x}, t)$ and $\rho_r(\vec{x}, t + \Delta t)$, after a time interval of Δt has passed assuming the dynamics (8). The second term accounts for diffusion and includes the discretization of the ∇^2 operator. This term includes positive and negative terms. The positive terms are contributions to the density at site \vec{x} from densities at neighboring sites. Neighboring sites are those sites which have the same coordinates as \vec{x} but for a single coordinate which must be only one lattice point away. This contribution is due the fact that diffusion causes chemicals to move from one location to another in space. The negative term accounts for the chemicals leaving site \vec{x} .

Now, if we replace f with the terms from the density field approach to reaction-diffusion, we get:

$$\begin{aligned} & \rho_r^*(\vec{x}, t + 1) - \rho_r^*(\vec{x}, t) = \\ & \Delta t \sum_{p=1}^l k_p N_{p,r} \prod_{s=1}^{s=m_p} \rho_{j_{s,p}}^*(\vec{x}, t) \\ & + \frac{D_r \Delta t}{\Delta x^2} (\rho_r^*(\vec{x} + (1, 0, \dots, 0), t) + \rho_r^*(\vec{x} + (-1, 0, \dots, 0), t) + \\ & \quad \rho_r^*(\vec{x} + (0, 1, \dots, 0), t) + \rho_r^*(\vec{x} + (0, -1, \dots, 0), t) + \dots \\ & \rho_r^*(\vec{x} + (0, 0, \dots, 1), t) + \rho_r^*(\vec{x} + (0, 0, \dots, -1), t) - 2d\rho_r^*(\vec{x}, t)) \end{aligned} \quad (11)$$

3 Microscopic Simulation of Reaction-Processes

3.1 Fundamentals of the Approach

In the previous section we have seen the prevailing approach for dealing with reaction-diffusion processes. Another approach that can be used is the microscopic simulation approach. This approach takes discretization one step further in the sense that the fields are discretized themselves, but takes a welcomed step backwards in the sense that time is not discretized. This approach is useful because it is closer to reality. Chemicals are discrete entities (at least in the classical approach which is a good approximation in solutions).

Again we have a field $\rho_r^{**}(\vec{x}, t)$ where $\vec{x} \in \omega^d$ $t \in \omega$, but this time $\rho_r^{**}(\vec{x}, t) \in \omega$. We have said that time is not considered discrete in the

microscopic simulation model, but nevertheless we have $t \in \omega$. This is not a contradiction it is simply an expression of the fact that reactions occur at discrete time points. Let us denote simulation discrete time with t^* and real time with t . Say the reactions occur, in the real system, at times t_n . Then when the simulation is at time $t^* = n$ it is supposed to approximate the real system at time t_n . Simulating the real system between the times t_n is of no use since nothing happens, except for diffusion which we should also treat as a reaction. But the problem is that diffusion, in the real system, is not a process that occurs at time points, rather it is a continuous process. On the other hand we have modeled space by discrete sites. Diffusion is modeled by chemicals hopping from one site to another. This process is discrete since chemicals hop at discrete time points. So amongst the times t_n there are times at which the reaction which takes place is diffusion, that is to say hopping of chemicals to neighboring sites. We should stress that the time interval between t_n and t_{n+1} is not a constant. So the real time is not approximated by $t^* \cdot \Delta t$ for some Δt .

The time interval between t_n and t_{n+1} is large when the time interval between successive reactions, in the real system, is large. Roughly speaking this happens when there are not many reactants, or many inert reactants. This is also when the microscopic simulation is at its best (in terms of the simulation's speed), since the simulation's single step covers a lot of time. We shall give a quantitative estimate for this time interval later.

Let us now turn to the relation of ρ^{**} to the real system that it is supposed to approximate. We assume space of dimensions d . Let us denote by $N_r(\vec{x}, l, t)$ the number of reactants, in the real system, of species r , located in a box of length l around \vec{x} at time t . The approximation relation is given below:

$$\rho_r^{**}(\vec{x}, t^*) \approx N_r(\Delta x \cdot \vec{x}, \Delta x, t_{t^*}) \approx \rho_r^*(\vec{x}, t_{t^*}) \cdot \Delta x^d n_0 \quad (12)$$

Let us imagine a grid of spacing Δx dissecting the real system, so that space is divided into little boxes. This division is not physical, but mental. Now each such box is simulated as a site on the simulation lattice. The number of reactants at each lattice point should approximate the number of reactants in a the little boxes imagined in the real system. This is the nature of the first approximate equality in equation (12) . The second approximate equality in equation (12) is due to the approximation of the finite difference approach to the real system.

3.2 The Monte-Carlo Method

Now we shall introduce the dynamics of ρ^{**} . Since the microscopic simulation is a Monte-Carlo simulation, ρ^{**} 's dynamics follow the following rules:

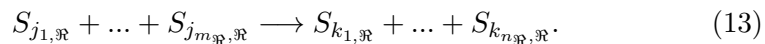
1. Choose $\rho^{**}(\vec{x}, t^* + 1)$ from a probability space, $\Omega_0(t^*)$.
2. Calculate the new probability space $\Omega_0(t^* + 1)$.

$\Omega_0(t)$ associates a probability for every possible $\rho^{**}(\vec{x}, t+1)$, but actually we are intent on performing one reaction at a time. So $\Omega_0(t)$ will give non-zero probabilities only for those $\rho^{**}(\vec{x}, t+1)$ that differ from $\rho^{**}(\vec{x}, t)$ by a single reaction (or diffusive hopping). So we can look at $\Omega_0(t)$ as associating a probability for every possible reaction. So let us construct a probability space $\Omega(\mathfrak{R}, t)$ which associates a probability for each possible reaction.

Let us speak of a reaction, \mathfrak{R} . This reaction can potentially take place anywhere in real space. In particular the reaction can fall within any one of the little boxes that we have discussed in the previous sub-section. We shall denote reaction \mathfrak{R} taking place at a little box corresponding to site \vec{x} by $\mathfrak{R}_{\vec{x}}$. Our task now is to find out, given some initial conditions, what is the probability that the reaction that will take place next is $\mathfrak{R}_{\vec{x}}$.

Let us expand a bit on the stochastic process that the real system undergoes. The stochastic process is comprised of events (reaction and diffusion) occurring stochastically at discrete time points. The events we are considering are the real reactions and the movement of reactants from one little box to an adjacent one. Let dt be a small time interval, then for $\mathfrak{R}_{\vec{x}}$ there is a chance $P(\mathfrak{R}_{\vec{x}}, t^*)dt$ that this reaction will occur in the time interval dt . The probability density, $P(\mathfrak{R}_{\vec{x}}, t^*)$, is called the reaction rate for reaction $\mathfrak{R}_{\vec{x}}$, and it is exactly what we used in order to formulate the PDE for the real system, as we shall soon see. First let us notice that this probability density has reciprocal time as units, which is consistent with the name 'rate'.

The connection of $P(\mathfrak{R}_{\vec{x}}, t^*)dt$ to the PDE's will be useful in calculating $P(\mathfrak{R}_{\vec{x}}, t^*)$. So let us explore this connection. Reaction \mathfrak{R} is of the form (1), that is to say:



A crucial assumption for the validity of the PDE's is that there is some time scale, dt , during which $P(\mathfrak{R}_{\vec{x}}, t^*)$ does not change much and still for the same time scale, dt , many reactions occur. Under these assumptions it can be shown that the number of reaction and diffusion events that occur

at the time interval dt in the box around \vec{x} is, simply, $P(\mathfrak{R}_{\vec{x}}, t^*)dt$. Let us look at species r (recall the notation used in equation (13)). Now let¹

$$N_{\mathfrak{R},r} = \#\{n|n \leq n_{\mathfrak{R}}, k_{n,\mathfrak{R}} = r\} - \#\{n|n \leq m_{\mathfrak{R}}, j_{n,\mathfrak{R}} = r\}. \quad (14)$$

This $N_{\mathfrak{R},r}$ gives the number of reactants of species r created in the reaction \mathfrak{R} (a negative number indicates that the species is annihilated in the reaction). So the number of reactants of species r formed, at the box around \vec{x} , in the time interval dt is:

$$P(\mathfrak{R}_{\vec{x}}, t^*) \cdot dt \cdot N_{\mathfrak{R},r} \quad (15)$$

The number of reactants of species r at the box which corresponds to site \vec{x} at time t_n is approximated by $\rho_r^{**}(\vec{x}, n)$. So the rate at which $\rho_r^{**}(\vec{x}, n)$ changes due to reaction $\mathfrak{R}_{\vec{x}}$ is given by:

$$\frac{\partial \rho_r^{**}}{\partial t}_{\mathfrak{R}_{\vec{x}}} = P(\mathfrak{R}_{\vec{x}}, t^*) \cdot N_{\mathfrak{R},r}. \quad (16)$$

Where the index $\mathfrak{R}_{\vec{x}}$ denotes that the reference is to the rate of change due to reaction $\mathfrak{R}_{\vec{x}}$ alone. We have already seen the rate of change in the finite difference case (equation (11)). There we expressed $\frac{\partial \rho_r^*}{\partial t}$ as a sum of terms, each expressing a rate due to different reactions. Another term was due to diffusion. Realizing that the terms appearing in the finite difference case express the same thing as the rate expressed at (16) modulo the approximation relation (12) we can find an expression for $P(\mathfrak{R}_{\vec{x}}, t)$, this is given by:

$$P(\mathfrak{R}_{\vec{x}}, t^*) = \Delta x^d n_0 \cdot k_{\mathfrak{R}} \prod_{s=1}^{s=m_{\mathfrak{R}}} \left(\rho_{j_{s,\mathfrak{R}}}^{**} \frac{1}{\Delta x^d n_0} \right) \quad (17)$$

This assumes that the reaction in question is a real reaction, that is not diffusion. For the case of diffusion of species l we have the following equation:

$$P(\mathfrak{R}_{\vec{x}}, t^*) = 2d \cdot D_l \cdot \frac{\rho_l^{**}}{\Delta x^d} \quad (18)$$

This equation is derived considering the last term in equation (11), $-\frac{2dD_r \Delta t}{\Delta x^2} \rho_r^*(\vec{x}, t)$, which is due to reactants hopping from site \vec{x} to neighboring sites. And then considering that $P(\mathfrak{R}_{\vec{x}}, t^*)$, in equation (18), is the probability density for hopping to neighboring sites. After using the approximation relation (12) we get (18).

¹#S denotes the number of elements in S.

Now that we have an expression for the rates $P(\mathfrak{R}_{\vec{x}}, t^*)$ of the different reactions, we still face the task of finding the probability associated with each possible reaction (including diffusion) by Ω . Again let us point out that the probability that Ω associates with reaction $\mathfrak{R}_{\vec{x}}$ at time t^* is the probability that this reaction will come next in the sequence of reactions. Now between the times t_{t^*} and t_{t^*+1} nothing happens in the reaction chamber, apart from reactants moving inside the little boxes we have imagined. In this time interval the reactants don't cross the boundaries of the boxes. If the rate of $\mathfrak{R}_{\vec{x},1}$ is twice that of $\mathfrak{R}_{\vec{x},2}$ then we should expect that reaction $\mathfrak{R}_{\vec{x},1}$ has twice the chance to be the next reaction that occurs than $\mathfrak{R}_{\vec{x},2}$. Let us expand a bit on the nature of the assumption we made in the previous statement. We assume that the probability distribution associated with Ω is dependent only on the situation of the current configuration of the reaction chamber and is independent of the time that passed since the last reaction-diffusion event. So it is actually this assumption (that the stochastic process has no memory) that allows us to compute the probability of different reaction and diffusion events associated by Ω as a function of the rates. The preceding argument leads to the following relation, given two reaction-diffusion events $\mathfrak{R}_{\vec{x},1}$ and $\mathfrak{R}_{\vec{x},2}$:

$$\frac{\Omega(\mathfrak{R}_{\vec{x},1}, t^*)}{\Omega(\mathfrak{R}_{\vec{x},2}, t^*)} = \frac{P(\mathfrak{R}_{\vec{x},1}, t^*)}{P(\mathfrak{R}_{\vec{x},2}, t^*)} \quad (19)$$

Taking into account the normalization of probability distribution to one, we now can compute the probability associated by Ω to a reaction-diffusion event $\mathfrak{R}_{\vec{x}}, t^*$. The solution is:

$$\Omega(\mathfrak{R}_{\vec{x},j}, t^*) = \frac{P(\mathfrak{R}_{\vec{x},j}, t^*)}{\sum_{\mathfrak{R}_{\vec{x},i}} P(\mathfrak{R}_{\vec{x},i}, t^*)}. \quad (20)$$

4 Anderson Localization in a Reaction-Diffusion System

4.1 The Reaction-Diffusion System

Anderson localization is a phenomenon associated with electron-transport behavior in disordered materials. The disorder in the material induces a phase transition of the electron eigen-functions from an unlocalized state in which Ohm's law is valid into a localized state in which the material behaves as an insulator. The wave functions of an electron under the influence of a periodic potential is periodic. A question arises, in the context of disordered materials, of how this periodic wave function is influenced by disturbances

to the periodicity of the potential. One might think that the eigenfunction of a slightly perturbed potential (that is to say perturbed from an originally periodic potential), would be eigen-functions slightly perturbed from a periodic function. This intuition proves misleading in the metal-insulator transition case. It is seen that some of the eigen-functions exhibit a marked departure from periodic functions, even for small disturbance of the potential. These functions are seen to be localized. Meaning that there are small “islands” in which the wave function has high modulus and there are large spaces between these islands where the wave-function has low modulus. Indeed the wave functions that depart from periodicity have the approximate form :

$$e^{-\frac{(x-x_0)}{\xi}} \quad (21)$$

ξ is the localization length of the eigenfunction. This approximation is good for the tails of the eigenfunction.

This Anderson localization effect is also observed in reaction diffusion system. Let us take the example given by Shnerb and Nelson. They presented a reaction-diffusion system described the schematics:



A is the only reactant to undergo diffusion.

Where \emptyset signifies that the reaction has no products (alternatively it can be interpreted that the products of the reaction are inert). These reactions together with diffusion can be seen as the schematics of the population biology of bacteria. The first reaction accounts for the reproduction of the bacteria. The rate at which the bacteria reproduce is controlled also by the concentration of F. F can represent, for example, the intensity of light that falls on the bacteria [20]. But can also represent any factor that controls the rate of bacteria reproduction, with the provision that this factor is not variable in time, and in particular non-exhaustible. The second reaction accounts for the dying of bacteria due to overcrowding. The reaction dynamics has the species **A** facilitating the production of more **A**'s. This property **A** is called autocatalysis. Autocatalysis is an important concept in pattern formation [23], the origins of life [5] [18] [3] [10] [1] and economy [22] (where autoctalysis is the underlying concept of multiplicative dynamics).

To see the similarity of this problem to an eigenfunction problem in quantum mechanics, such as Anderson localization, let us write down the

PDE's which are associated with the reaction dynamics above:

$$\frac{\partial \rho_A}{\partial t} = D_A \nabla^2 \rho_A + \rho_A \cdot \rho_F - \rho_A^2 \quad (23)$$

which can be reformulated into:

$$\frac{\partial \rho_A}{\partial t} = (D_A \nabla^2 + \rho_F - \rho_A)(\rho_A) \quad (24)$$

Now if we drop the last term, we have:

$$\frac{\partial \rho_A}{\partial t} = (D_A \nabla^2 + \rho_F)(\rho_A) \quad (25)$$

which is quite analogous to the time dependent Schrödinger equation:

$$i \frac{\partial \psi}{\partial t} = \left(\frac{1}{2m} \nabla^2 + U(x, t) \right) (\psi) \quad (26)$$

Where we have U playing the part of ρ_F , $\frac{1}{2m}$ playing the part of D_A and ψ playing the part of ρ_A . We have only to remember that we have dropped the quadratic term and that there is an additional coefficient, $-i$, in the Schrödinger equation ². Consequently, the reaction-diffusion PDE, without the quadratic term, can be seen as a Schrödinger equation with imaginary time.

Notice that we did not write an equation for $\frac{\partial \rho_F}{\partial t}$ since ρ_F does not undergo any dynamics and therefore does not change in time. The phenomena of Anderson localization determines that if ρ_F is not constant in space, but rather is stochastic, then we shall have these localized states that we have described above, both for the quantum mechanics case and for the reaction-diffusion case. In the quantum mechanics case, a constant or periodic potential, $U(x, t)$, entails a periodic field, ψ . In the reaction-diffusion case, a constant potential, ρ_F , entails a constant field, ρ_A .

A constant, stochastic potential naturally arises when speaking of disordered materials [19]. But in reaction-diffusion systems, such a potential is more of a stretch. We have given the example of light intensity as a stochastic constant potential. But in many more cases the reaction rate associated with the reproduction of bacteria, or some chemical, is dynamic. This leads us to deal with a dynamic potential, $U(x, t)$. Nelson and Shnerb have already discussed a time-dependent potential of the form $U(x - vt)$ (actually they have looked at the case where the media is moving, which is equivalent to a moving potential in the opposite direction).

² i here is $\sqrt{-1}$

4.2 Results of microscopic simulations for Anderson localization

We simulated (using microscopic simulation) the reaction dynamics associated with Anderson localization . The reaction schematics (together with the reaction rates) is given below³:

1. $\mathbf{A} + \mathbf{C} \rightarrow \mathbf{A} + \mathbf{A} + \mathbf{C}$ (15)
2. $\mathbf{A} + \mathbf{A} \rightarrow \emptyset$ (3)
3. $\mathbf{A} \rightarrow \emptyset$ (60)

The size of the reaction chamber is 300x300 lattice points. The average number of molecules of type \mathbf{C} per site is 5. They are dispersed in the beginning of the simulation randomly. That is to say that the positions of the 5x300x300 molecules of type \mathbf{C} are chosen at random. The spatial distribution that resulted can be seen in figure (1). The initial distribution of \mathbf{A} is similarly dispersed but with an average of 2 molecules of type \mathbf{A} per site. Only \mathbf{A} molecules diffuse. The simulation's diffusion rate is 3. After awhile a steady state is reached. Off-course \mathbf{C} is not dynamic, and it remains as in figure (1). On the other hand \mathbf{A} is dynamic and the steady state is depicted in figure (2)

4.3 Anderson Localization - in the search of dynamic clustering

Shnerb and Nelson[20] have explored the consequences of changing the potential $U(x)$ by a moving potential $U(x - vt)$, what would happen if instead of having the potential drift at a constant speed the potential would undergo diffusion itself? This would correspond to replacing (23) by the two coupled equations:

$$\begin{aligned} \frac{\partial \rho_A}{\partial t} &= D_A \nabla^2 \rho_A + \rho_A \cdot \rho_F - \rho_A^2 \\ \frac{\partial \rho_F}{\partial t} &= D_F \nabla^2 \rho_F \end{aligned} \quad (27)$$

We have found no treatment in the literature for this kind of moving potential for a good reason: if ρ_F is treated as non-negative continuous

³The numbers in parentheses at the right of the reactions denote their corresponding rates

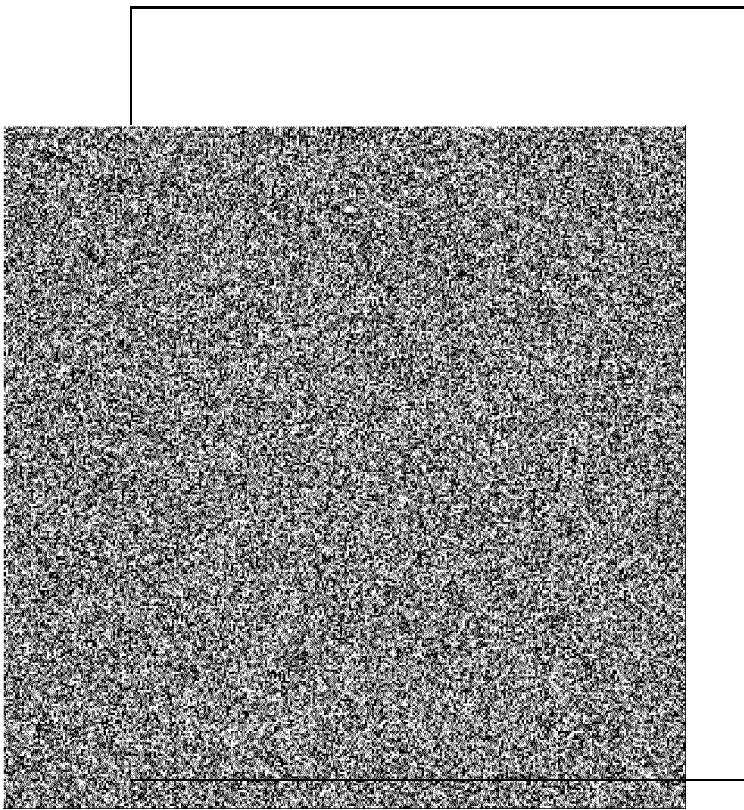


Figure 1: Snapshot of molecules of type **C**.

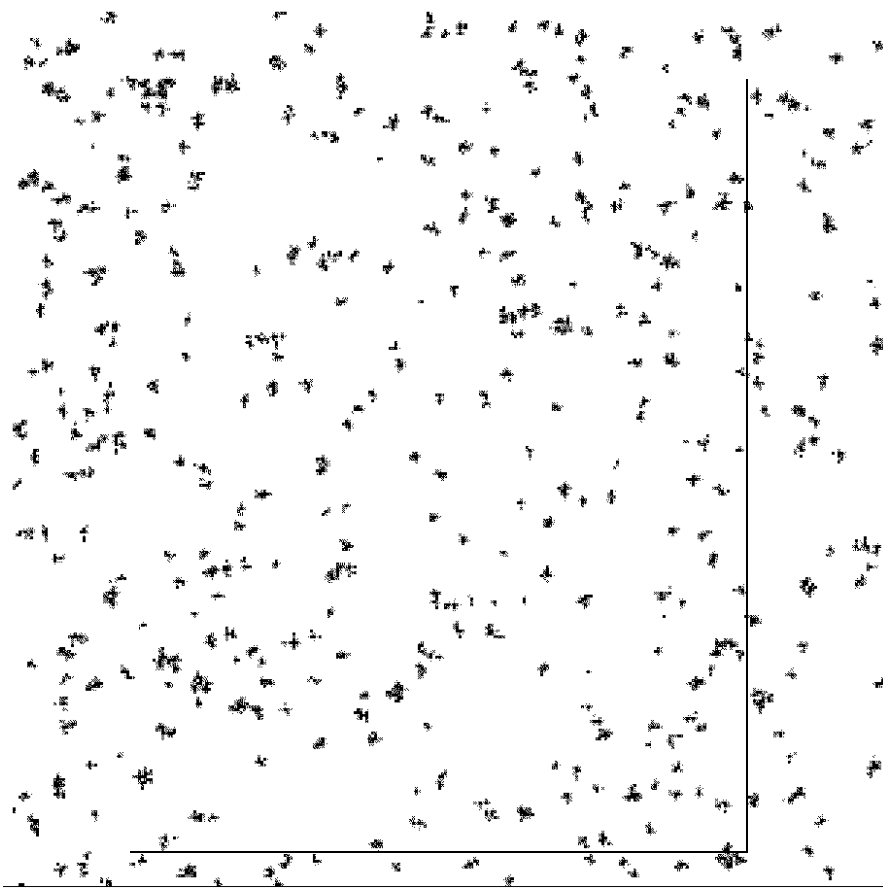
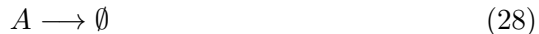


Figure 2: Snapshot of molecules of type A.

variable as is usually done in the context of differential equations and since the only dynamics imposed on ρ_F by (27) is diffusion, ρ_F converges to a steady spatially-uniform state $\rho_F = \text{const}$, giving rise to the trivial solutions of a system with no potential fluctuations at all. But if the potential is treated as a discrete variable diffusion does not necessarily induce the uniform distribution of the potential and localization effects still have a chance to prevail. This situation leads to clear differences between the different simulation approaches we have described, in further sections we will show other examples in which discretization leads to different results in different simulation methods.

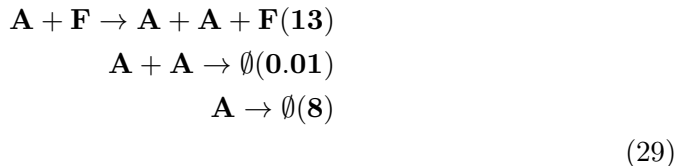
Extending the analogy to population biology we could look at \mathbf{A} as representing a population of parasites dependent on a host species \mathbf{F} for a-sexual reproduction. The population represented by \mathbf{F} is not affected by the parasites and performs random diffusion in space. The phenomena we are most interested in is dynamic clustering or grazing. Dynamic clustering would under our analogy represent parasite herds moving in space due to changes in the spatial distribution of the species they need in order to reproduce.

Translating our situation into a reaction-diffusion system will give the same results as (22) but in this case both \mathbf{A} and \mathbf{F} undergo diffusion. We have added to (22) the reaction:



representing the dying of \mathbf{A} not due to overcrowding.

Since (22) describes no creation or elimination of \mathbf{F} the total number of \mathbf{F} s in all the lattice sites is constant throughout the simulation and $\langle \mathbf{F} \rangle$ - the average concentration of \mathbf{F} is constant as well. Given a constant value for D_A the results of simulations of (29) are controlled by $\langle \mathbf{F} \rangle$ and D_F . We have simulated (using microscopic simulation) the following reaction-diffusion system with different values of $\langle \mathbf{F} \rangle$ and D_F and keeping $D_A = 6$:



The size of the simulation is 128x128. The system was seeded with 3 reactants of species \mathbf{F} per cell and 1 reactant of species \mathbf{A} per cell (the reactants were placed at random locations).

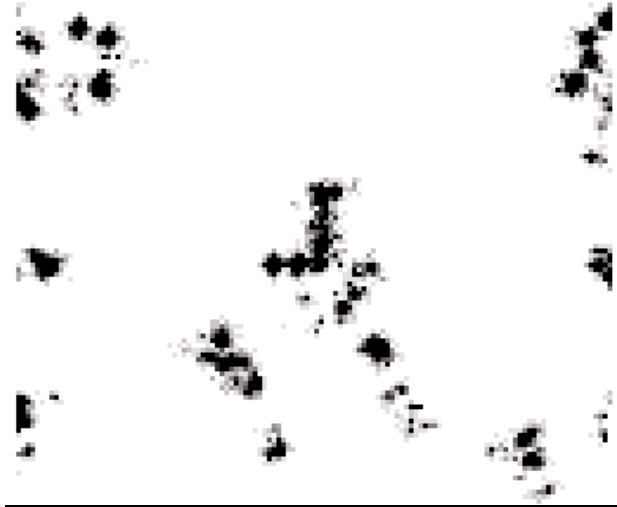


Figure 3: Snapshot of \mathbf{A} 's concentration, simulation parameters are $D_A = 6, D_F = 4, \langle \mathbf{F} \rangle = 0.15$.

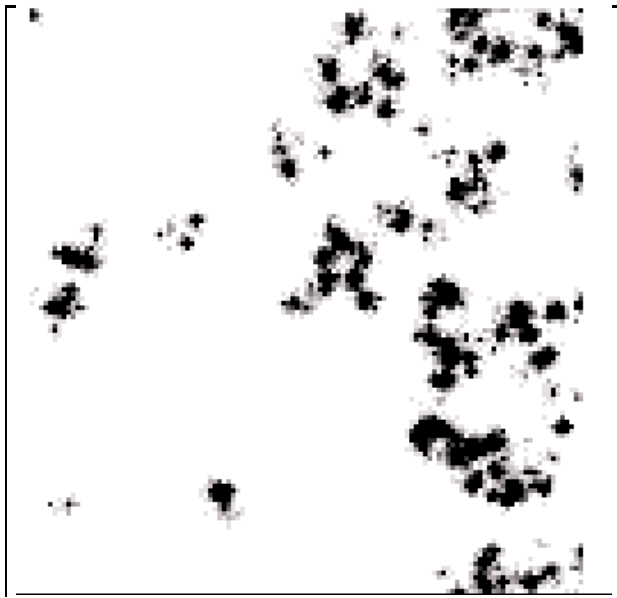


Figure 4: Snapshot of the same simulation as in (3) at a later time, the clusters have moved. The result of this simulation falls into the β category in our notation.

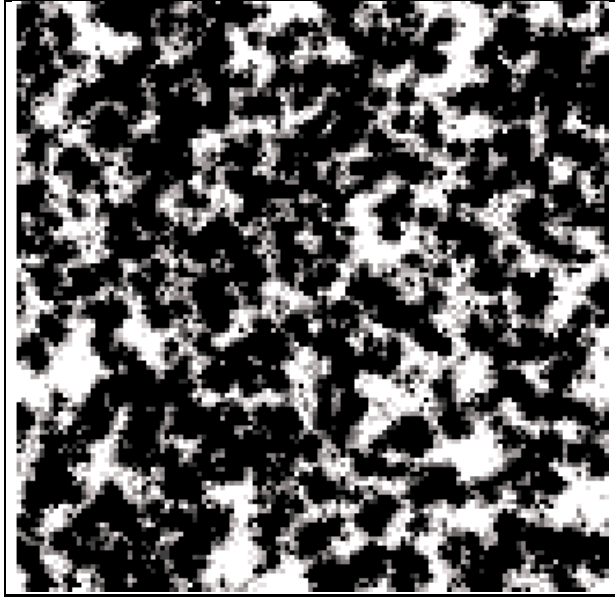


Figure 5: **A**'s fill up the simulation space, this corresponds to a γ situation in our notation.

We have divided the results of the simulation into 3 categories:

- α - The simulation results in **A** filling the whole simulation space.
- β - The simulation results in **A** forming dynamic clusters.
- γ -The simulation results in the total extinction of **A** from the simulation space.

In fig(7) we can see an abrupt phase-transition between α states to γ states for high D_F values around $\langle F \rangle = 0.61$. We shall give a theoretical explanation to this phase change. For high D_F values **F** reactants take shorter times to pass between different parts of the simulation space. Therefore we can assume that **A** reactants are affected by all **F** reactants in the simulation space and the mean-field approximation:

$$F = \langle F \rangle \tag{30}$$

is valid.

⁴Numbers in parentheses at the right of reactions are the corresponding reaction-rates.

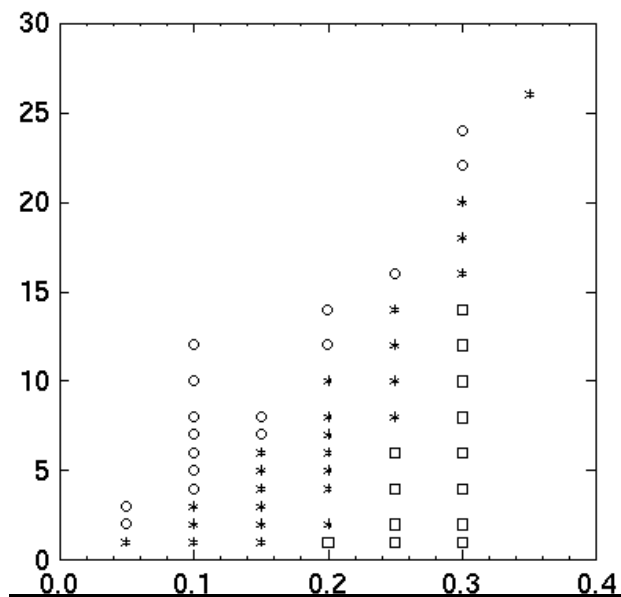


Figure 6: Results of simulations of the system(29) for different values of $\langle \mathbf{F} \rangle$ (x-axis) and D_F (y-axis). Notice that dynamic clustering occurs also in the realistic range of: $0.5D_A < D_F < 1.5D_A$. Circles denote simulation resulting in α situations, Asterisks denote simulations resulting in β situations and squares denote simulations resulting in γ situations.

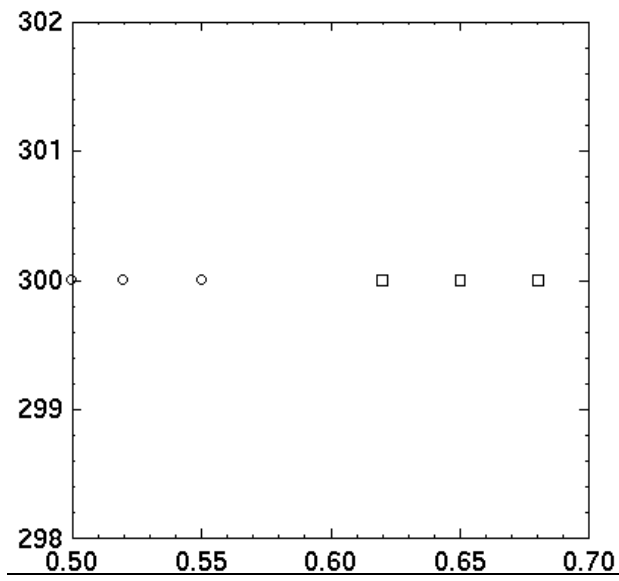


Figure 7: Results of simulations of the system(29) for $D_F = 300$ (y-axis) as a function of $\langle F \rangle$ (x-axis), circles denote simulations ending in an α situation and squares denote simulations ending in a γ situation. The change in behavior is abrupt and occurs in the 0.55-0.61 region. Simulations in that parameter region resulted in β situations.

Assuming (30) we are now looking for solutions to:

$$\frac{\partial \rho_A}{\partial t} = D_A \nabla^2 \rho_A + k_1 \rho_A \cdot \langle F \rangle - k_2 \rho_A^2 - k_3 \rho_A \quad (31)$$

Keeping in mind that \mathbf{A} can take only integral values and dropping the diffusion term from (31) we find that:

$$\langle F \rangle = \frac{k_2 + k_3}{k_1} \quad \mathbf{A} = 1 \quad (32)$$

is an unstable node fixed point of (31). This leads to predict the death of \mathbf{A} s for $\langle F \rangle$ smaller than $\frac{k_2+k_3}{k_1}$ and that \mathbf{A} s fill up the space for $\langle F \rangle$ larger than $\frac{k_2+k_3}{k_1}$.

In the case of the simulated set of reactions (29) we have:

$$\frac{k_2 + k_3}{k_1} \approx 0.61 \quad (33)$$

The preceding argument explains the sharp transition between α and γ states for the high $D_F = 300$ value as can be seen in fig(7).

One might be tempted to think that this mean-field argument will be sufficient in explaining the emergence of grazing at low D_F values: for low diffusion coefficients persistent spatial discrepancies in \mathbf{F} 's concentration prevail throughout the simulation space, some areas would be affected from a local \mathbf{F} concentration larger than 0.61 and would sustain a population of \mathbf{A} s and some areas with a lower local \mathbf{F} concentration would be empty of \mathbf{A} s. These spatial discrepancies change with time causing our clusters to move across the simulation space. If this was the sole mechanism leading to the grazing behavior one would expect that the β simulation results would appear for low D_F values equally distributed on both sides of the $\langle F \rangle = 0.61$ asymptote. Clearly, fig(6) shows us that this is not the case, the β situations are concentrated around lower and lower $\langle F \rangle$ values as D_F decreases. Therefore we should search for another mechanism in order to explain the behavior seen in fig(6). For lower D_F values, D_A is not negligible and clusters are not only supported by an influx of \mathbf{F} reactants, but are also supported by their own ability to move and “find” areas of high \mathbf{F} concentration in their surroundings. This mechanism of “searching” for \mathbf{F} reactants should be part of an explanation for the behavior seen in fig(6) at low D_F values.

5 Microscopic simulation of the Gray-Scott model

5.1 The Gray-Scott model - a pattern formation mechanism

The Gray-Scott model[9] was first designed as a model of glycolysis and as in the simplest form of Turing[23] pattern formation it involves two reactants one of them enhancing the auto-catalysis of the other, but the geometrical patterns resulting from this model are different from the ones observed in the Turing pattern case and unlike the Turing pattern case pattern formation occurs when diffusion coefficients are equal as well. The model is given by:

$$\begin{aligned}\frac{\partial \rho_C}{\partial t} &= \nabla^2 \rho_C - \rho_C \rho_A^2 + F(1 - \rho_C) \quad , \\ \frac{\partial \rho_A}{\partial t} &= D_A \nabla^2 \rho_A + \rho_C \rho_A^2 - (F + k) \rho_A\end{aligned}\quad (34)$$

where $\rho_A(\vec{x}, t)$ and $\rho_C(\vec{x}, t)$ are the concentration fields for two chemical reactants **A** and **C** respectively. The terms $F(1 - \rho_C)$ and $-(F + k)\rho_A$ in (34) describe the system as being in contact with an external reservoir kept at $\rho_C = 1$ and $\rho_A = 0$. Indeed (34) accepts the solution:

$$\begin{aligned}\rho_C &= 1 \\ \rho_A &= 0\end{aligned}\quad (35)$$

Consider the equations that result from (34) by dropping the diffusion terms. The above mentioned stable fixed point exists throughout parameter space but for some range of **F** and **k** Pearson[15] has found another fixed point. Fixing **k**, increase or decrease of **F** causes the second steady state to be lost. The process of losing or gaining fixed-points as a function of the system's parameters is called bifurcation. Looking at the non-diffusive system's behavior under change in the external parameters can be very useful in order to understand the general behavior of the diffusive-system under microscopic simulation.

Two types of bifurcations are usually distinguished - saddle-node bifurcation and Hopf bifurcation.

In a saddle-node bifurcation either a fixed point appears and splits into two fixed points or two fixed points become one and then disappear. The main feature of such bifurcations is the nature of the single fixed point at the bifurcation. The linearized system must have one zero eigenvalue and one non-zero eigenvalue at that point. In other words if

$$\frac{\partial f(\vec{t})}{\partial t} = \mathbf{M}f(\vec{t})\quad (36)$$

is the linear expansion of the system around the fixed point, with \mathbf{M} being the 2x2 coefficient matrix, then at the bifurcation point $\det(\mathbf{M}) = 0$ and $\text{tr}(\mathbf{M}) \neq 0$.

Hopf bifurcation occurs when an unstable (stable) focus goes through the creation of a limit cycle and becomes stable (unstable). At the bifurcation point both eigenvalues are purely imaginary and the Real part of the eigenvalues is positive (negative) before the bifurcation point and negative (positive) after the bifurcation point.

In the case of our system, given \mathbf{k} the second fixed point is lost through saddle-node bifurcation as \mathbf{F} is increased and by Hopf bifurcation as \mathbf{F} is decreased.

Pearson [25] considers ρ_C as the density of a liquid fuel and ρ_A as a temperature field. Fuel is constantly fed from an external reservoir kept at a constant concentration. The fixed point in (35) is stable therefore small perturbations in the temperature field around the zero will tend to die out and return back to the zero, but what if the perturbation was big enough (a match is thrown into the fuel) to cause the term $\rho_C \rho_A^2$ to be significant?

Here the auto-catalytic nature of (34) would cause temperature and fuel consumption to increase inside the ignited area and the fire starts spreading across space, leaving regions with low concentrations of fuel. Given the feed parameters \mathbf{F} and \mathbf{k} the behavior is controlled by the value of D_A . Large values of D_A would cause fast moving fire wavefronts and small values of D_A cause stable standing spots of fire fueled by the fast moving \mathbf{C} . One of the more interesting patterns arising from (34) is that of replicating spots predicted in simulations [15] and confirmed in experiment [16]. Given the right parameter values an initial large perturbation breaks up into standing spots, the fuel concentration at the middle of the spot decreases and causes the spot to divide into two smaller expanding replicas and so on.

Analytic spot-like solutions to (34) were found in [25] but only in the one-dimensional case and in the $D_A \ll 1$ limit.

The different two-dimensional patterns resulting from the Euler integration of (34) were classified in [15].

5.2 Reproducing the replicating spots phenomenon in microscopic simulations.

The following equations :

$$\frac{\partial \rho_C}{\partial t} = 2 \cdot 10^{-5} \nabla^2 \rho_C - \rho_C \rho_A^2 + 0.018(1 - \rho_C)$$

$$\frac{\partial \rho_A}{\partial t} = 10^{-5} \nabla^2 \rho_A + \rho_C \rho_A^2 - 0.074 \rho_A \quad (37)$$

fall in the parameter space domain described by Pearson[15] to produce the replicating spots behavior. Pearson has used lattice-spacing of 0.01 and has started his simulation in the trivial state: $\rho_A = 0$, $\rho_C = 0$ apart from the perturbed square put at: $\rho_A = 0.25$, $\rho_C = 0.5$. The reaction dynamics corresponding to equation (37) are:

1. $\mathbf{A} + \mathbf{A} + \mathbf{C} \rightarrow \mathbf{A} + \mathbf{A} + \mathbf{A}(\mathbf{1})$
2. $\mathbf{A} \rightarrow \emptyset(\mathbf{0.74})$
3. $\mathbf{C} \rightarrow \emptyset(\mathbf{0.018})$
4. $\emptyset \rightarrow \mathbf{C}(\mathbf{0.018})$

The simulation space (of size 64x64 sites) is seeded with 1000 \mathbf{C} s and no \mathbf{A} s, except for the perturbed square (of size 20x20 sites) that is seeded with 250 \mathbf{A} s per cell and 500 \mathbf{C} s per cell. n_0 was chosen to be 10^7 and lattice spacing was chosen to be 0.01 (so a concentration of 1 corresponds to 1000 reactants per lattice site).

Although we have been successful in reproducing the general replicating spots behavior, a closer look at the results as shown in figures (9) and (8) shows that the randomness introduced in the microscopic simulation has the effect of breaking the square symmetry preserved by the PDE simulations. Pearson originally achieved this symmetry breaking by introducing noise in the initial conditions, but the same effect is created by the microscopic simulation. Figure (10) shows the results of the simulation at a later time, replication has formed more spots. Figure (11) shows the results of a PDE simulation of the same system. We can see the similarity in the results of the two simulations, due to the fact that n_0 is large. We shall see, in the next subsection, that when other parameters are chosen (including n_0), the two systems give crucially different results.

5.3 The uniqueness of persistently dynamic reaction-fronts to microscopic simulation.

We now present an example in which microscopic simulations of the Gray-Scott model create different results than the ones obtained by the PDE approach. The phenomenon we are interested in is the presence persistent reaction fronts propagating through the simulation space. Much research has been devoted to reaction fronts [6][8][14][24][12]. Patterns which are

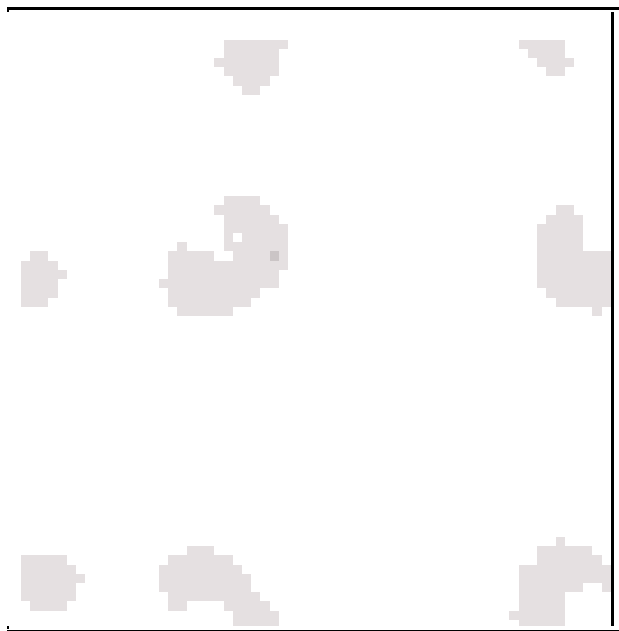


Figure 8: Replicating spots of \mathbf{A} created by the microscopic simulation. Spots in the process of dividing are shown.



Figure 9: The same simulation as in fig(8) at a later time, the original spots have split in two.

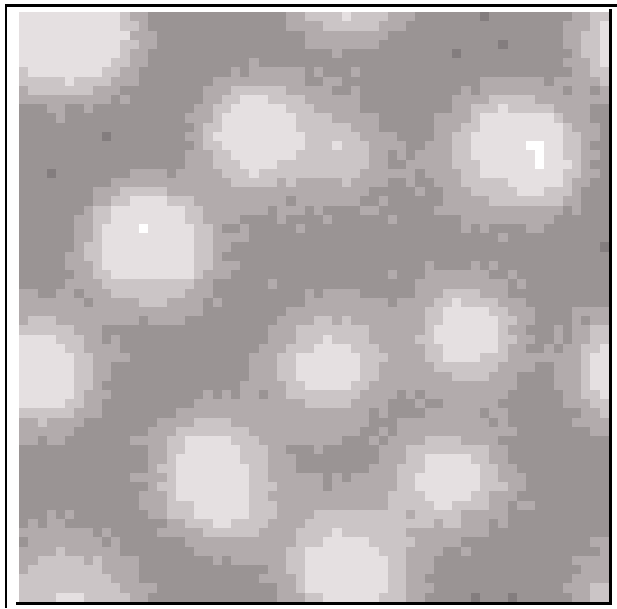


Figure 10: The same simulation as in fig(9) and (8) but at a later time. This figure shows species **C**.

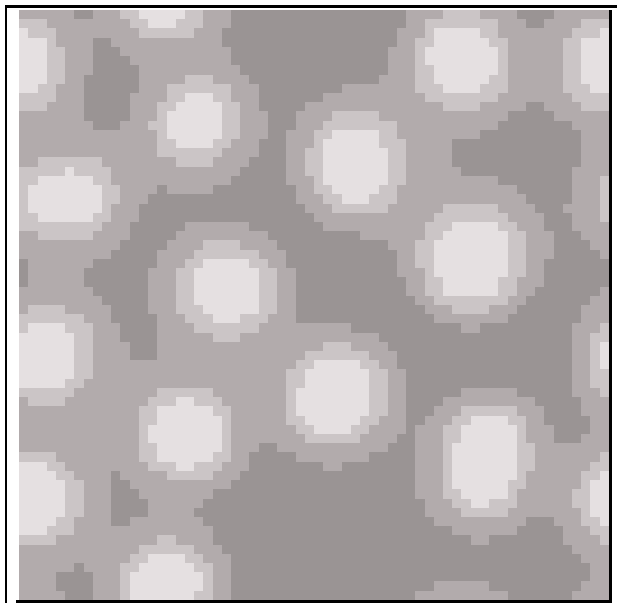


Figure 11: This figure shows results of PDE simulation of the replication spots. Again showing species **C**.

non-stationary in time and inhomogeneous in space at the same time are rare in a homogeneous medium. We suggest a system where the reaction-fronts are spatially and temporally non-stationary within a homogeneous medium (all the participating reactants have non-zero equal diffusion rates, so the system is not equivalent to a non-homogeneous medium system). Our persistent reaction-fronts are created by the following mechanism: A localized small **A** area consumes **C** reactants in its surroundings and creates reaction-fronts of high **A** concentration propagating across the simulation space cleaning areas from the presence of **C**s. The reaction-front then runs out of high **C** concentration areas and decays, giving rise to the renewal of **C**s and new wavefronts produced by the surviving **A**s and so on. We have simulated microscopically the following reaction-diffusion system:

1. $\mathbf{A} + \mathbf{A} + \mathbf{C} \rightarrow \mathbf{A} + \mathbf{A} + \mathbf{A}(\mathbf{8})$
2. $\mathbf{A} \rightarrow \emptyset(\mathbf{0.3})$
3. $\mathbf{C} \rightarrow \emptyset(\mathbf{0.02})$
4. $\emptyset \rightarrow \mathbf{C}(\mathbf{0.1})$

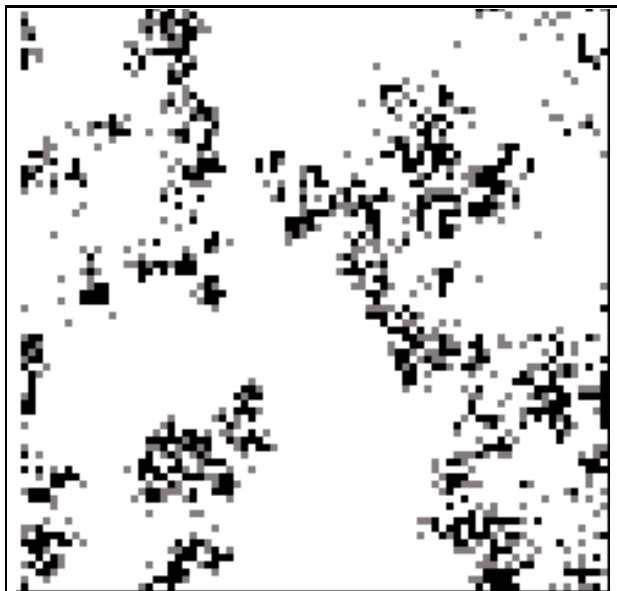


Figure 12: Clear high **A** concentration reaction-fronts can be seen during microscopic simulations. These reaction-fronts are persistent, being supported by surviving **A** reactants.

The diffusion coefficients are $D_A = 1$ and $D_C = 1$. The simulation size chosen was 80×80 . $n_0 = 1$ and $\Delta x = 1$. The simulation space was seeded with 1 **C** per site, and no **A**'s were seeded except for a perturbed square of size 64×64 sites where 5 reactants of species **A** per site were seeded. The simulation shows persistent reaction-fronts of the type seen in fig(12).

Using Euler Integration to simulate the system we get different results, the initial square perturbation does propagate in the form of a reaction-front shown in fig(13), but after the initial front cleans the space from high **C** concentration areas the front decays and gives way to the total elimination of **A**s from the simulation space. Unlike the microscopic case in which the discretization and randomness leave behind some islands of **A** from which the next reaction-front can emerge, the Euler Integration drives the system towards the $\rho_A = 0$ steady-state. Introducing noise in the initial conditions does not change the situation the system tends to smooth out these noises and is driven to the constant steady state.

We have tried to reproduce the persistent reaction-fronts pattern using Euler Integration with no success, although it is plausible that the same behavior will appear for high values of n_0 .

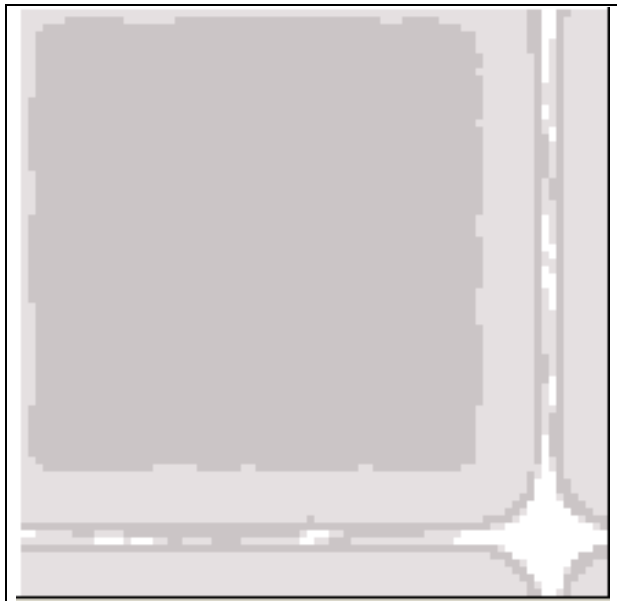


Figure 13: The initial reaction-front seen when integrating the corresponding PDE system with $\Delta x = 1$ and $n_0 = 1$. The reaction-front dies out and the system is driven to the constant $\rho_A = 0$ steady-state.

6 Microscopic simulation of Marketing models

6.1 Using rate equations to describe the marketing of products

The application of physical sciences methods to economic and financial research, nowadays common practice among the scientific community[17], was initiated by the work of Bachelier[11] and Mandelbrot[4]. The basic situation is similar to the other areas of research we have previously discussed, global “macroscopic” economic phenomena are generated by the underlying “microscopic” process of buy and sell. Under these circumstances it is natural to try and use microscopic simulation of market models in order to reproduce as an example we could take the spreading of steam engines or gunpowder starting from localized innovative centers and sweeping across wide regions of the globe.

When using microscopic simulation to describe product marketing one can regard a lattice-space element in two different ways:

1. As a geographical region - neighborhood, town or country.
2. As a business entity - company or corporate.

In the first case neighboring elements represent geographically close regions, in the latter case they represent companies that are in business contact. The reactants could stand for any kind of valuable passing from one place or business entity to another. One could have reactants representing money, products, ideas, manpower or technology. Reactions could represent economic processes in which valuables are transformed, lost or created. Diffusion stands for the transfer of these valuables from one location or business entity to another. Although the use of microscopic simulations in the context of marketing seems natural enough there still are some flaws to point at and points to defend. The microscopic simulation is probabilistic in nature while some of the processes we try to represent are deterministic. As we explained in previous sections rates represent the occurrence rate of an underlying Poisson process for some of the economic processes described we have no reason to think that they are Poissonic in nature. Furthermore the microscopic simulation’s lattice-space elements are always connected with exactly 4 neighboring sites, thus disabling the simulation of environments in which the degree of “connectedness” varies from site to site. If we consider sites to be business entities as we have previously suggested, we certainly would like to consider different amounts of connectivity between business entities - a feature not supported by the microscopic simulation system.

6.2 The “Tamagotchi” model

In collaboration with J. Goldenberg and D. Mazursky⁵ we have devised the following set of reactions:⁶

1. $\mathbf{B} + \mathbf{C} \rightarrow \mathbf{A} + \mathbf{B} + \mathbf{B}(\mathbf{8})$
2. $\mathbf{A} \rightarrow \emptyset(\mathbf{0.7})$
3. $\mathbf{B} \rightarrow \emptyset(\mathbf{1.5})$
4. $\emptyset \rightarrow \mathbf{C}(\mathbf{0.1})$
5. $\mathbf{C} \rightarrow \emptyset(\mathbf{0.02})$

The inspiration to these reaction dynamics comes from the wave of “Tamagotchi” games we have been subjected to during a short period of 1996. These reaction dynamics were simulated in a system of size 128x128 sites seeded with 1 reactant of species **C** only. A square of size 64x64 sites was seeded with 1 reactant of species **C** per cell and 5 reactant of species **B** per cite. Other coefficients are: $n_0 = 1$, $\Delta x = 1$.

- **A** - represents a product (“Tamagotchi”).
- **B** - represents the idea or concept of the product.
- **C** - represents money.

In this model neighboring locations should be interpreted in the geographical sense. The only diffusing reactant is **B** with diffusion coefficient **1** but since **B** represents an idea or concept the diffusion it performs is replicative. By replicative we mean that instead of hopping from one cell to a neighboring cell a copy of the original reactant is created and planted in the neighboring cell. This replicative diffusion represents the fact that ideas or concepts do not physically pass from one location to another, instead a location exposed to a new idea or concept in a neighboring location creates its own copy of the original idea. In terms of the microscopic simulation algorithm the only change is that when executing the diffusion of **B**, a **B** unit is added to the target location but none is subtracted in the original location. The first reaction represents the following process: A person exposed to the product concept that is in possession of money spends the money

⁵Hebrew University School of Business Management

⁶Numbers at the right of reactions are the corresponding reaction-rates.

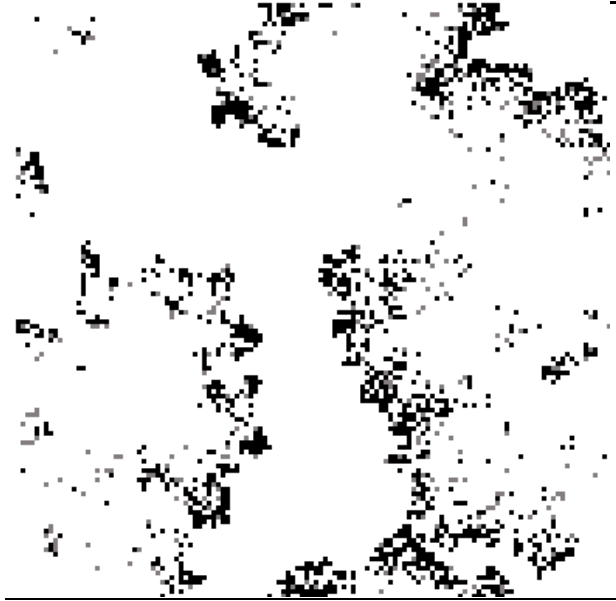


Figure 14: Snap shot of A 's concentration clear wavefronts can be seen. Sites with concentration above 2 are drawn black.

on buying the product and a new concept or idea of the product is “born” in that persons mind. The second reaction represents the loss of products due to old age. The third reaction represents the fact that ideas tend to be forgotten. The fourth reaction represents an influx of money and the fifth reaction represents the spending of money on products other than A . The “replicative” diffusion that B undergoes represents the influence ideas have on neighboring locations.

6.3 Wave fronts the “Tamagotchi” model

During the simulations of the “Tamagotchi” model we have observed long lasting wavefronts of high A concentrations moving across the simulation space. The process giving rise to such waves seems to be the following: Starting with a small amount of A in a C rich area the concepts created by this small A concentration propagate to neighboring sites and induce the decrease of C concentration and increase in A concentration in these sites. The areas to which this B influence arrives then become C poor areas stopping the increase in A 's concentration giving rise to their decrease until C 's concentration is high enough to sustain the next wavefront.

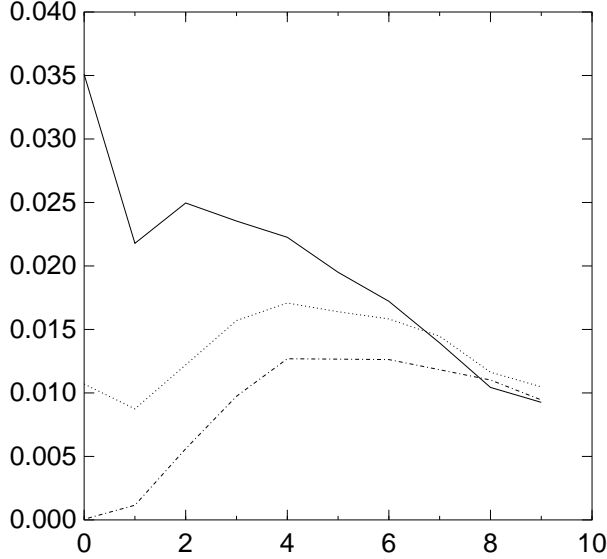


Figure 15: $C(r, t_0, t)$ plotted as a function of r for $t=3,4,5$, the higher the plot the lower is t . A clear 'hump' can be seen to advance in r as t increases, corresponding to the evolution of the wavefront.

In order to estimate the propagation speed of the wavefronts we have used the following correlation integral. Let Ω denote our two-dimensional reaction chamber and let $\rho_A(\vec{x}, t)$ denote the concentration of \mathbf{A} at location \vec{x} and time \mathbf{t}_0 for $\vec{x} \in \Omega$ and $\mathbf{t}_0 \geq \mathbf{0}$. For $\mathbf{r} \geq \mathbf{0}$ let:

$$V(\Omega) = \int_{\Omega} 1 d\vec{x} \quad (38)$$

$$\mathbf{C}(r, t_0, t) = \frac{1}{V(\Omega)} \int_0^{2\pi} \int_{\Omega} \rho_A(\vec{x}, t_0) \rho_A\left(\vec{x} + \begin{pmatrix} r \cos \theta \\ r \sin \theta \end{pmatrix}, t_0 + t\right) d\vec{x} d\theta - \frac{1}{V(\Omega)^2} \int_{\Omega} \rho_A(\vec{x}, t_0) d\vec{x} \int_{\Omega} \rho_A(\vec{y}, t_0 + t) d\vec{y} \quad (39)$$

Given $\mathbf{t} \geq \mathbf{0}$ and $\mathbf{r} \geq \mathbf{0}$ (39) is a measure for the correlation between \mathbf{A} 's concentration at time \mathbf{t}_0 and \mathbf{A} 's concentration at time $\mathbf{t}_0 + \mathbf{t}$ at locations with distance \mathbf{r} . If ρ_A is static $C(r, t_0, t)$ is maximal for $\mathbf{r} = \mathbf{0}$ for all \mathbf{t} s. If on the other hand ρ_A is moving at speed \mathbf{v} we expect for a given \mathbf{t} that C is maximal for $\mathbf{r}=\mathbf{v}\mathbf{t}$.

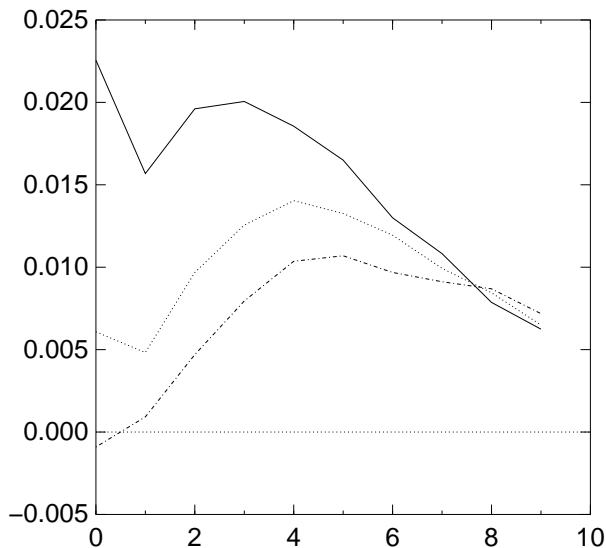


Figure 16: $C(r, t_0 + 50, t)$ plotted as a function of r for $t=3,4,5$, the higher the plot the lower is t . The same 'hump' as in (15) although t_0 has increased by 50.

In both (15) and (16) we can see an increase of 2 in r as t increases by 2 giving rise to an estimate of:

$$v \approx 1 \tag{40}$$

When speeds are measured in units of lattice-sites per simulation-time. The similar approximations due to the different choices of t_0 indicate the constant speed of advance of the wavefront.

7 Acknowledgment

We wish to thank Sorin Solomon for instructing us in this work. We thank Jacob Goldenberg and David Mazursky their help in finding the application to marketing. We also thank Nadav Shnerb for fruitful discussions.

References

- [1] A.I. Oparin. *The origin of life on the earth*. Oliver and Boyd, London, 1957.

- [2] J. Nagumo, S. Arimoto and S. Yoshizawa. *Proc. IRE*, 50:2061, 1962.
- [3] A.S. Kauffman . *The origins of order - Self-organization and selection in evolution*. Oxford University Press, Oxford, 1993.
- [4] B. Mandelbrot. *Journal of Business*, 35:392, 1963.
- [5] F. Dyson. *Origins of Life*. Cambridge University Press, Cambridge , Great Britain, 1985.
- [6] R. J. Field and M. Burger. *Oscillations and Traveling Waves in Chemical Systems*. Wiley, New York, 1985.
- [7] R. A. FitzHugh. *Biophys. J.*, 1:445, 1961.
- [8] J. S. McCaskell, G. J. Bauer and H. Otten. *Proc. Natl. Acad. Sci. USA*, 79:737, 1989.
- [9] P. Gray and S.K. Scott. *J. Phys. Chem.*, 89:22, 1985.
- [10] A.S. Kauffman. *At Home in the Universe: the search of the laws of complexity*. Viking, 1995.
- [11] L. Bachelier. *Annales Scientifiques de l'Ecole Normale Supérieure*, 3(17):21, 1900.
- [12] S. Kadar, L. Lengyel and I.R. Epstein. *Phys. Rev. Lett.*, 9:2729, 1992.
- [13] H. Levy, M. Levy and S. Solomon. *J. Phys. France*, 1087, 1995.
- [14] Q. Ouyang and H. L. Swinney. *Chaos*, 1:1411, 1991.
- [15] J. E. Pearson. *Science*, 261, 1993.
- [16] J. E. Pearson and H. L. Swinney. *Nature*, 369:215 , 1994.
- [17] R. Cont, M. Potters and J.P. Bouchaud. *Scale invariance and Beyond*. Springer, Berlin-Heidelberg, 1997. Edited by B. Dubulle, F. Graner and D. Sornette.
- [18] D. Segre and D. Lancet. A statistical chemistry approach to the origin of life. *Chemtracts 1998 - Special Issue on the Chemistry of Life's Origin, in press*.
- [19] B. I. Shkolovskii and A. L. Efros. *Electronic Properties of Doped Semiconductors*. Springer-Verlag, N. Y., 1984.

- [20] N.M. Shnerb and D.R. Nelson. *cond-mat/9708071*, 1997.
- [21] J.M. Smith. *Mathematical Ideas in Biology*. Cambridge University Press, Cambridge, Great Britain, 1968.
- [22] S. Solomon and M. Levy. *Int. J. Mod Phys. C*, 7:745, 1996.
- [23] A. Turing. *Philos. trans. R. Soc. London B*, 237:37, 1952.
- [24] J. Boissonade, V. Castets, E. Dulos and P. De Kepper. *Phys. Rev. Lett.*, 64:2953, 1990.
- [25] S. Ponce-Dawson, W. N. Reynolds and J. E. Pearson. *Phys. Rev. E*, 56:1, 1997.